J. Synchrotron Rad. (1996). **3**, 260–267

Studies of the Structure of Matter with Photons from an X-ray Free-Electron Laser

S. Doniach

Departments of Applied Physics and Physics, Stanford University, Stanford, CA 94305, USA

(*Received 23 April 1996; accepted 17 July 1996*)

X-ray free-electron lasers offer the potential for fourth-generation ultra-high peak power and coherence X-ray beams in the hard X-ray (8 keV) spectral range. A critical review of three areas of potential application of such sources is presented. Owing to the enormous electric field strength at the focus of such beams, it is shown that matter would very rapidly form a plasma for focal spots of submicrometer dimensions. Thus, hologram formation would only be feasible for crystalline samples with dimensions of a few micrometers or greater. A new version of X-ray holography using interference between a sample and a reference two-dimensional crystal is proposed. Because of the very high peak intensity of the free-electron-laser pulses, a natural application is to time-resolved multibunch 'dynamic X-ray scattering' measurements. It is shown that this could provide information on dynamical processes in condensed matter complementary to that obtained using slow neutron beams. Finally, optical laser-induced pump-probe-type experiments are reviewed. There is the potential for extending the study of the charge distribution of electronic excited states to those with lifetimes in the submillisecond time range.

Keywords: free-electron laser; X-ray holography; laser plasma generation; X-ray parametric scattering; dynamic X-ray scattering; time-resolved studies; fourth-generation sources.

1. Introduction

Given an X-ray free-electron laser (FEL) operating at ångström wavelengths as is being proposed for the LCLS (linear coherent light source) at SLAC (Arthur, Materlik & Winick, 1994; Arthur, Materlik, Tatchyn & Winick, 1995), what new information about the structure of matter may be obtained relative to that already accessible with current synchrotron radiation sources? The aim of this report is to provide a critical overview of three areas of experimentation: potential for X-ray holography, dynamic X-ray scattering (time-resolved fluctuation measurements), and laser-induced X-ray parametric scattering. We show that for measurements involving time resolutions faster than a few milliseconds, the LCLS offers qualitative advantages over X-ray undulator sources. The very high brightness of X-ray FEL sources, on the other hand, may only present an advantage in very special circumstances.

2. Characteristics of the photon beam from the LCLS – comparison with output from X-ray undulators at third-generation storage rings

In order to evaluate the range of measurements over which the LCLS would present new opportunities, a comparison with alternative X-ray sources is required. Here we make a comparison with X-ray undulators on third-generation machines such as the APS or ESRF.

The raw beam pulse from the X-ray LCLS has $\sim 5 \times 10^{12}$ photons at 8 keV delivered in ~ 65 fs (Arthur *et al.*, 1994, 1995). The bandwidth is in the few eV range (~ 5 eV) and the repetition rate is 120 Hz. The average brightness, 10^{21} photons (s mm^2 mrad^2 0.1% bandwidth)$^{-1}$, is such that it could, in principle, be focused down to a spot size of the order of ~ 2 Å. (Actually, the beam size is ~ 9 μm at the exit of the undulator with a transverse divergence of 2 μrad.) Similar figures have been given for a proposed X-ray FEL at DESY, Hamburg (Rossbach, 1996).

For comparison with an X-ray undulator on a 6–8 GeV machine an average spectral brightness of $\sim 5 \times 10^{18}$ photons s^{-1} (10 eV bandwidth)$^{-1}$ (mm^2 mrad^2)$^{-1}$ can be used. Substituting phase-space parameters for a 5 m undulator at the APS of 0.02 mm^2 × 200 μrad^2 would give an average photon count of $\sim 10^{15}$ photons (10 eV)$^{-1}$ s^{-1} exiting the undulator. A comparison of total flux is not very meaningful since what really matters is the number of photons delivered to a sample, which depends on details of the beam optics in a given experiment. However, for some idea of the comparison of the two kinds of X-ray source, one may estimate that the average delivered photon flux from the LCLS, based on a repetition rate of 120 pulses s^{-1}, is about the same as (or maybe a factor of two over) an equivalent bandwidth taken from an APS undulator. Recent LCLS studies suggest that about ten micropulses could be delivered per linac macropulse, which could yield a total flux an order of magnitude greater than that available from an APS undulator (H. Winick, personal communication).

The big difference, of course, is in the number of photons per pulse. Assuming the APS repetition rate is of the order

of 10^6 s^{-1} (which will depend on the bunch structure in the ring), the LCLS will deliver 10^4 more photons per pulse. Thus, an advantage is to be had in situations where time-resolved measurements are to be made on a time scale where the X-ray undulator pulses fall short of the desired photon flux delivered.

To assess the relative usefulness in single-bunch mode, more detailed considerations are needed. For instance, if a triggering event, *e.g.* a photochemical reaction, can only be set off once per second, then for time-resolved measurements under times needed for 10^4 X-ray undulator pulses, *i.e.* ~ 10 ms, there will be an advantage in using the LCLS. A factor which needs to be considered in this context is degradation of the sample, since the advantage of the LCLS can be compensated for by signal averaging over many event cycles.

We show below (§6) that use of the LCLS in two-bunch or multibunch mode could provide a new way to explore sub-terahertz excitations in condensed matter through post-detector interferometry, as in dynamic light scattering. We propose that 'dynamic X-ray scattering' could open up a new area of experimentation which could explore in a complementary way some of the properties of matter hitherto accessible only through the use of slow neutron diffraction.

Another important potential difference between the LCLS and undulator sources is for applications needing a high degree of coherence. One example is in the measurement of the relaxation of critical fluctuations near a second-order phase transition (see §6). Here it is desirable to achieve scattering-vector resolutions of the order $\delta q/q \cong 10^{-5}$. For an undulator–sample distance of 20 m this would mean using an X-ray optic set-up which would only utilize $\sim 4\,\mu m^2$ of the source area. Within this resolution this would reduce the average power by a factor of the order of 10^{-4}. Since the LCLS beam can, in principle, be focused down to a spot with a size on the ångström scale, the resolution of the LCLS beam would be of the order $\delta q/q \cong 10^{-10}$ and would have ample resolution for the experiment. Thus, for a class of high-resolution measurements of this kind, the LCLS might have a 10^4-fold advantage, even based on average power. Similar or greater advantages might be gained for measurements of laser-induced parametric X-ray scattering (see §9).

3. Maximum usable field strength at the focus of the LCLS beam

A frequently discussed idea in FEL applications (London *et al.*, 1992) is that a hologram image of a biological sample could be caught in an instant before the sample vaporizes (Solem & Baldwin, 1982). Since the LCLS coherence is such that the beam could, in principle, be focused down to a waist size of ångström dimensions, one may ask whether it might be possible to capture holograms of a single molecule. Here we argue that the instantaneous electric field strengths at the focus of an LCLS pulse are so large that the sample will turn into a plasma and the resulting forces will disrupt the atomic structure within a few femtoseconds.

What is the energy density of X-rays which would be needed to make a hologram of a single molecule? 300 coherently scattered photons per atom is a reasonably conservative estimate, as may be seen from the following very rough argument. To measure Bragg peak intensities in a protein crystal to an accuracy of 10%, ~ 100 photons per Bragg peak would be needed. For a small protein of 100 amino acids, one has $\gtrsim 1000$ atoms and needs to collect on the order of 3000 Bragg peak intensities (in practice more like 10 000). This works out to at least 300 photons per atom. However, the diffraction is over the whole crystal so that any one molecule in the crystal only sees relatively few photons.

To see a single molecule, enough X-ray intensity needs to be focused to yield 300 coherently scattered photons per atom. Taking the coherent cross section of nitrogen as 6.5 b (1 b = 100 fm^2) and the radius of the atom as 1.5 Å, this means one needs to shine at least 3×10^9 photons on each atom to make a hologram. If these are delivered in 50 fs, then the energy density approaches 2×10^{20} erg cm^{-3} (1 erg cm^{-3} = 10^{-1} J m^{-3}), giving an electric field strength of $\sim 6 \times 10^5$ V Å^{-1}.

How long will atoms survive at these field strengths? The following argument suggests that they will form a plasma in a few hundred attoseconds (10^{-18} s; as). Consider an electron in a Bohr orbit. The X-ray E-field hits it with force impulses of alternating sign at the X-ray frequency (a period of 1 as^{-1} for a 3 Å wavelength X-ray). The velocity of the electron therefore oscillates by eE/m per cycle. For an electron in free space this averages to zero. However, for an electron in a Bohr orbit, it instantaneously reaches escape velocity within 1 as for orbits for which the binding energy is of the order $\beta^2\varepsilon_H$, where $\beta = eEa_B/\hbar\omega$ with a_B the Bohr radius (0.5 Å), $\hbar\omega$ the X-ray energy, and ε_H = 1 rydberg (2.17 aJ). Since the electron still has its orbiting velocity, this will add to the instantaneous oscillating velocity induced by the electric field, and the electron will drift away from the nucleus. For $\beta = \mathcal{O}(10)$, this means all the outer-shell electrons will be stripped away in a Bohr orbit period which will be on the scale of a few hundred attoseconds. Thus, by this very simple argument, which may be thought of as the classical limit of an 'inverse bremsstrahlung' mechanism, we may estimate that a high-temperature electron plasma, whose energy will be characterized by the drift velocity of the electrons in their Bohr orbits, *i.e.* of the order (~ 100 eV, $\sim 10^6$ K), will be formed in less than 1 fs. This very crude estimate is in fact born out by more sophisticated calculations (More, Zinamon, Warren, Falcone & Murnane, 1988; Rozmus, Tikhonchuk & Cauble, 1996). A second mechanism for heating the atomic electrons, that of longitudinal radiative momentum transfer (*i.e.* photon pressure), has been pointed out by Tatchyn (personal communication). This acts through the A^2 coupling to the electromagnetic field as opposed to the $\mathbf{j}\cdot\mathbf{A}$ term invoked above. However, a simple

estimate suggests that this term will contribute a heating rate to the electron gas of a couple of orders of magnitude smaller than that produced by the first mechanism.

Since for low-Z elements the coherent X-ray scattering cross section is mainly from the outer electrons, this will tend to obscure the atomic information after the atoms are ionized. At this stage the ion cores will start to experience strong forces and also become a plasma. The rate at which the ions heat up is much more difficult to estimate. One may conjecture that electric fields generated by the electron plasma will couple directly to the ions. A carbon nucleus will move $\sim 1/3$ Å fs^{-1} in an electric field of 100 V Å^{-1} (caused by the electron plasma, not the X-rays). Recent estimates (Rozmus, Tikhonchuk & Cauble, 1996) suggest that ionic heating may be quite rapid. Hence, it seems very likely that the molecule will form a plasma within a few fs, *i.e.* before the residual ions can yield a useful diffraction pattern.

What about diffraction from a single molecule taken at lower field strengths (*i.e.* over many pulses)? This is still problematic since the photoelectron cross section of *e.g.* nitrogen is 1.6×10^2 b at 8 keV, *i.e.* about 26 times greater than the coherent X-ray cross section.

One has to conclude that X-rays from the LCLS can only observe molecular structure on ångström scales if the X-ray scattering is coherently superposed from many molecules arranged in a periodic array, *i.e.* a crystal. Application of the holographic idea may still be of interest in this context since it can, in principle, produce a solution of the phase problem of X-ray crystallography.

4. Holography at ångström length scales

Holography, or 'lensless photography', comes in two varieties: Fresnel or Gabor holography, in which the diffracted beam interferes with a plane-wave incident beam, and Fourier holography, in which the diffracted beam interferes with a divergent beam. In Gabor holography the fringe spacing is set by the scale of the X-ray wavelength, so a direct application of this kind of holography is detector-resolution limited and hence is not practical at ångström length scales (Solem, Boyer, Haddad & Rhodes, 1990). It has, however, been rather successfully exploited for soft X-rays at resolutions of the order of 50 nm (Lindaas, Jacobsen, Howells & Frank, 1992; Kirz *et al.*, 1994).

In X-ray Fourier holography a diverging reference beam is required which is most straightforwardly generated by diffracting from a reference scatterer or array of scatterers. In fact, this is the basis of the standard method of phasing by isomorphous replacement in protein crystallography. Recently, there have been some interesting developments where X-ray fluorescence radiation has been exploited as a point source (Tegze & Faigel, 1996) or a near-field detector (Gog *et al.*, 1996). The first of these techniques, which still requires the presence of an array of heavy atoms in the crystal, leads to a far-field image in q space, which potentially alleviates the need to measure many separate Bragg reflections as is done in rotation camera measurements for protein crystallography. It will be interesting to see if these methods can be extended to apply to macromolecular crystals. Here we discuss yet another possible holographic technique based on diffraction from a two-dimensional reference crystal.

Suppose one has a thin film of disordered two-dimensional crystallites of a polymer [a convenient recently measured example is that of poly-3-hydroxybutyrate (Mahendrasingam *et al.*, 1995)]. The diffracted beam from such a film will be a powder pattern in the form of concentric cylinders in reciprocal space. Each cylinder may be thought of as made up of stripes corresponding to the Bragg rods resulting from diffraction from a given crystallite in the film. To each rod there will be a set of corresponding rods resulting from diffraction from the same crystallite. In practice, because of disorder in the polymer crystal (see below) and disorder in the protein crystal, both the Bragg rods from the polymer and the Bragg spots from the protein will have a finite width. If the X-ray beam passing through this film is simultaneously diffracted from a protein crystal, then by adjusting the orientation of the crystal relative to the normal to the film, it should be relatively easy to find a condition such that two Bragg spots from the crystal simultaneously intersect, at least partially, with two Bragg rods from the same crystallite in the film.

This may be seen as follows: by tilting the film relative to the crystal one guarantees that the scattering vector $\mathbf{G}_P$ of one of the protein Bragg reflections is commensurate with a vector $(\mathbf{g}_f, k_z)$ of one of the Bragg rods, where $\mathbf{g}_f$ is a two-dimensional Bragg rod of the polymer film. Then the projection of the protein inverse lattice on the plane of the film will contain a set of symmetry-related Bragg spots of the protein lying on a circle around the $(0, 0, k_z)$ cylinder axis. Since the tilt angle has found a commensurability condition for one of the film Bragg rods, there will also be a set of symmetry-related Bragg rod projections on the same circle. Because the protein unit-cell dimensions are quite a bit larger than those ($\sim 5 \times 6$ Å) of the polymer, and because of the finite width of the rods and spots, it seems likely that there will generally be some overlap. Given the unit-cell dimensions, a computer search of the overlapping reciprocal spaces can be made to find the best sets of reflections with which to measure the resulting interference effects.

Provided the film–crystal assembly can be held rigid to a precision of the order of ångströms during rotations, then the intensities of the pairs of Bragg spots which are simultaneously interfering with rods from the appropriate two-dimensional crystallite may be measured as in standard X-ray crystallography.

Technically, the experiment will require a double-axis orientation of the crystal relative to the film normal by a set-up which may subsequently be rotated as an integral assembly for the crystallographic measurement. Because the crystallites making up the polymer film need to be all oriented to a rather close tolerance within the film plane,

it seems likely that the area of exposure of the reference film to the X-ray beam will be quite small, maybe of the order of tens of micrometers. For maximum contrast of the interference of X-rays diffracted by the film with those from the protein crystal, both should have roughly the same total number of atoms in the beam. Hence a microfocus X-ray beam will be important. Such beams are of course already available at the ESRF. Coherence requirements for this kind of measurement are not more restrictive than in conventional protein crystallography. The only fundamental advantage at the LCLS would therefore be for time-resolved measurements.

One imponderable in this proposal is the degree of two-dimensionality of the polymer crystallites. Since the simultaneous intersection of the Bragg spots with the rods will in general mean that k_z along the rod will be different between the two Bragg spots from the protein, it will be important to have an accurate calibration of both phase and amplitude of the diffraction profile as a function of k_z along each rod, which would be obtained by an atomic scale model of the crystal structure of the polymer crystal unit cell. However, if the unit cell is very elongated along the film plane normal, then it may be expected to have many kink-like defects which would smear out this k_z scattering profile. This is not in itself a disadvantage provided the resulting average phase and amplitude can be accurately determined, which is an experimental question. The other general difficulty will come from the need to measure the degree of overlap of the simultaneously diffracting rods and spots, since the interference effects will scale with this overlap. Further research will therefore be required to find out whether the proposed holographic technique can be useful.

If these various difficulties can be overcome, the phasing of that subset of Bragg reflections for which pairs largely satisfy the simultaneous diffraction conditions with pairs of rods will result by measuring the change of intensities relative to those taken in the absence of the polymer film, as in usual isomorphous replacement experiments, and correcting for the overlap factors as discussed above. It should be noted that since only a relatively small number of Bragg reflections could be potentially phased by this method, it can only provide a limited solution to the phase problem. Nevertheless, this might be sufficiently useful that it could provide an adjunct to the more conventional phasing methods based on heavy-metal derivatives or on multiple anomalous diffraction.

5. Time-resolved protein crystallography

What is the limit of smallness for a protein crystal whose X-ray diffraction could be measured by the LCLS? To drive the local E-field strength β factor down to, for example, 0.01, would increase the spot size to $\sim 1000\,\text{nm} = 1\,\mu\text{m}$. Assuming unit-cell dimensions of $\sim 30\,\text{Å}$, a crystal of this size would contain $\sim 4 \times 10^4$ protein molecules. Since there are $\sim 5 \times 10^{12}$ coherent photons in one LCLS pulse, this would result in $\sim 10^7$ coherently diffracted photons per pulse. The accompanying ionization damage would amount to $\sim 7 \times 10^3$ photoionization events per protein molecule or more than one per atom, which would certainly destroy the crystal in one pulse, but maybe not faster than would be needed to collect a diffraction signal. For a $10\,\mu\text{m}^3$ crystal the damage per LCLS pulse would be reduced to $\sim 2 \times 10^2$ events per molecule, which might be low enough to allow more than one shot per crystal.

To judge how this would compete with an X-ray undulator beam one must realize that the LCLS beam is of relatively low bandwidth ($\sim 5\,\text{eV}$) while the undulator radiation can be used in Laue scattering mode and exploit a larger bandwidth by maybe an order of magnitude. Hence, one needs to consider the practical aspect of the number of reflections which can be captured per rotation setting of the protein crystal, which is greater in the Laue mode than in the monochromatic mode. Typically, only a few tens of reflections could be seen per LCLS pulse, leading to a need for reduced photon flux per pulse in order to reduce the radiation damage per pulse to acceptable levels.

6. Dynamic X-ray scattering

The availability of a source of intense pulses of X-rays would make attractive an extension to X-ray wavelengths of the dynamic (*i.e.* time-resolved) light-scattering technique (Berne & Pecora, 1990) for measuring time-dependent fluctuations in matter. In this section we give examples of what kinds of information could be obtained using this 'dynamic X-ray scattering' (DXS) technique.

Excluding resonant scattering, the scattering of X-rays is well described by the Thompson cross section for which the relevant scattering cross section with wavevector $\mathbf{q}$ at time t may be expressed in terms of

$$S_q(t) = \rho_q(t)\rho_{-q}(t), \tag{1}$$

where ρ_q is the electron number density operator

$$\rho_q = \sum_i \exp(i\,\mathbf{q}\cdot\mathbf{r}_i), \tag{2}$$

summed over all electrons in the sample including inner- and outer-shell electrons.

The dynamic scattering experiment may then be written in terms of the four-point correlation function

$$I(q,q',\tau) = (1/T)\int_0^T \mathrm{d}t\,\langle \rho_q(t)\rho_{-q}(t)\rho_{q'}(t+\tau) \times \rho_{-q'}(t+\tau)\rangle. \tag{3}$$

In practice the measurement is made by post-detector interferometry in which a scattering cross section is measured with a first X-ray pulse at time t, wavevector $\mathbf{q}$, and a second cross section at wavevector $\mathbf{q}'$, time $t + \tau$, is measured

with a second X-ray pulse at a time τ later than the first measurement.*

Provided τ is large compared with the X-ray oscillation period, the quantum mechanical interference between the two X-ray measurements may be neglected so that the measurement process when averaged numerically over many pairs of observations should be a good approximation to the general expression in (3).

To understand the physics of this measurement, we first consider a classical limit in which $\rho_q(t)$ is written in terms of atomic coordinates

$$\rho_q(t) = \sum_i \exp\,[i\,\mathbf{q}\cdot\mathbf{R}_i(t)], \tag{4}$$

where $\mathbf{R}_i$ is a set of atomic positions.

We can then express the four-point correlation function as a product of two-point functions plus an irreducible part

$$\begin{aligned} I(q,q',t) = {} & \langle \rho_q \rho_{-q}\rangle\langle \rho_{q'}\rho_{-q'}\rangle \\ & + \langle \rho_q(0)\rho_{q'}(t)\rangle\langle \rho_{-q}(0)\rho_{-q'}(t)\rangle \\ & + \langle \rho_q(0)\rho_{-q'}(t)\rangle\langle \rho_{-q}(0)\rho_{q'}(t)\rangle + I_{\text{irred}} \end{aligned} \tag{5}$$

where I_{irred} is defined by this equation and, for a system in equilibrium, the time average is absorbed into the ensemble average.

For a translationally invariant system such as a liquid we have

$$\langle \rho_q(0)\rho_{-q'}(t)\rangle = \delta_{q,q'} S_q(t)\ , \tag{6}$$

with

$$S_q(t) = \langle \rho_q(0)\rho_{-q}(t)\rangle = \left\langle \sum_{i,j} \exp\,\{i\mathbf{q}\cdot[\mathbf{R}_i(0) - \mathbf{R}_j(t)]\}\right\rangle. \tag{7}$$

In the limit that cross-correlations are neglected by setting $I_{\text{irred}} = 0$ [the so-called Gaussian approximation (Berne & Pecora, 1990)], we then have the basic result

$$I(q,q',t) \cong \delta_{q,q'}[S_q^2(0) + S_q^2(t)]. \tag{8}$$

It is interesting to note that two separate scattering measurements are actually measuring an interference function between different atoms $\mathbf{R}_i$, $\mathbf{R}_j$ at different times. This seemingly bizarre 'post-detection interferometry' phenomenon (the equivalent of laser speckle in light scattering) makes use of the fact that the measurement is made quickly enough so that the phase difference between X-rays scattered from a pair of atoms has not yet had time to randomize. In fact, the experiment measures this randomization time through the decay of $S_q(t)$.

Note that the coherence requirements on the X-ray beam are rather low, defined by the q-space resolution of the measurement. In the particular case of very slowly relaxing critical fluctuations measured by Stephenson and collaborators (Brauer *et al.*, 1995; Sutton *et al.*, 1991) (time scale of thousands of seconds), coherence is important since the length scale of the relevant fluctuation is of the order of micrometers. However, for fast events such as macromolecular conformation changes, the coherence requirements would be much less stringent. A critical question which would need to be answered for this type of experiment is that of stability from bunch to bunch: some method would need to be developed to calibrate the beam intensity for each bunch in order to allow for accurate post-detector interferometry.

The time scales of phenomena measured by DXS would depend on the repetition rate available for X-ray pulses. On an undulator beam like at a storage ring, the fastest times readily accessible would be of the order of microseconds or fractions of a microsecond (for multibunch mode). In principle, faster times could be accessed by ultra-fast time-resolved detection within a single storage ring bunch with duration of the order of 1 ns. On the LCLS, the natural bunch spacing in multibunch mode would be set by the 3 GHz klystron frequency, thus of order 300 ps. Shorter delays could be caused by splitting the beam and introducing a delay (perhaps using multilayer monochromatic mirrors). It is also noteworthy that the underlying SASE (self-amplification by stimulated emission) mechanism of the X-ray FEL intrinsically generates a very rapid subfemtosecond time structure (Bonifacio, De Salvo, Pierini, Piovella & Pellegrini, 1994) which could, in principle, be exploited for very short time scale DXS.

The constraints on short time measurement would probably be set by detector response times, since the experiment is based on counting photons separately at times t and $t + \tau$. To get down to picosecond time resolution will therefore present a challenge to detector designers. Time-resolved measurements on the LCLS could naturally extend out to the 0.1–1 μs bunch length of the linac.

An example of an application in the tens of nanoseconds would be to observe helix $\leftrightarrow$ random coil transitions in small polypeptides. Current laser-induced temperature-jump experiments are reporting transition rates in the 30 ns or so range, measured through time-resolved IR absorption experiments (Williams *et al.*, 1996). X-ray scattering could add additional understanding by giving time-resolved information on changes in radius of gyration and possibly other shape indicators. A limitation here would be the decay of the signal due to molecular diffusion. A small protein would diffuse an r.m.s. distance of 2 nm in ~6 ns, thus blurring q-space information for shorter q. This could be slowed down by observing the molecules in a high-viscosity medium such as glycerol. A somewhat similar example, which has already been studied by the technique of slow neutron spin-echo spectroscopy, is that of internal polymer chain Brownian motion, on the tens of nanoseconds time scale, in small star-shaped micelles made from block co-polymers (Farago *et al.*, 1993).

* Note that the 'heterodyne' mode of measurement used in dynamic light scattering, in which the scattered signal is mixed with a feed from the main beam, would not work for X-rays from the LCLS. Here the poor longitudinal coherence (*i.e.* in the time domain) is indicated by the bandwidth (~ 10 eV) of the LCLS X-rays.

7. Comparison of relative advantages of X-ray FELs and third-generation storage ring sources for DXS

By the use of 'time-tagged photons', DXS measurements on a submicrosecond time scale are already possible in principle at third-generation storage ring sources. It is therefore of interest to make a direct comparison of the relative advantages of the FEL compared with a storage ring source. In particular, by filling a storage ring with trains of electron bunches spaced by times of the order of nanoseconds, it will be possible to consider DXS measurements on these time scales.

Consider an X-ray scattering channel with wavevector **q** in which there are N_q photon counts s^{-1}. By recording the arrival time of each photon, *i.e.* time-tagging the photon scattering events, it will be possible to evaluate the time delays between every pair of photon scatterings and sort these into bins. For simplicity, we suppose that there are m bunches in a bunch train, with a train repetition rate of $R_S\ s^{-1}$. Then there are $N_b = N_q/mR_S$ photon counts per bunch in channel q. The resulting number of correlated photon events spaced by a multiple- of one-bunch spacing is of the order $n_c = 2N_b^2 mR_S = (2N_q^2/R_S m)\ s^{-1}$.

Compare this with an X-ray FEL source which has the same average number of photons s^{-1} but now concentrated into trains of m bunches with train repetition rate R_F. The number of photons per bunch in the given scattering channel is now $N_b = N_q/R_F m$. The number of correlated scattering events resulting from a pair of bunches is then $n_c = (2N_q^2/R_F m)\ s^{-1}$. Hence the relative effectiveness of the FEL compared with the storage ring will be $n_c|_F/n_c|_S = R_S/R_F$. For instance, if the storage ring repetition rate is $10^6\ s^{-1}$ and that of the FEL is $100\ s^{-1}$, and it is assumed that the FEL and storage ring both lead to the same average count rate per channel, then the FEL has an intrinsic advantage of 10^{-4} resulting from the compression of the photons into short pulses relative to the storage ring photon bunches which come out many more times per second but with much lower peak power per bunch.

8. Observing terahertz electronic charge-density excitations in superconductors

If sub-picosecond time-resolution measurements can be made on the LCLS (modulo detector limitations as discussed above), then a new area of charge-density spectroscopy could be opened up. We consider here the case of charge-density excitations in a superconductor.

The charge-density operator for a conduction band may be written

$$\rho_q = \sum_{k,\sigma} c^\dagger_{k+q,\sigma} c_{k,\sigma} \ . \tag{9}$$

In a BCS ground state this may be rewritten in terms of Bogoliubov–Valatin operators *via*

$$c^\dagger_k = u_k \alpha^\dagger_k + v_k \alpha_{-k} \ . \tag{10}$$

Then ρ_q couples directly to a pair of quasi particles

$$\rho_q = \sum_k u_{k+q} v_k \alpha^\dagger_{k+q} \alpha^\dagger_{-k} + (\text{particle} - \text{hole terms}) \ . \tag{11}$$

The Cooper-pair operator $\alpha^\dagger_k \alpha^\dagger_{k'}$ would have a bound state with binding energy of the order of the superconducting energy gap. This would be the charge density analog of the 41 meV neutron peak seen in YBCO which may be interpreted as a triplet Cooper-pair resonance (Demler & Zhang, 1995). This will then lead to an oscillatory response for $S_q(t)$ with a period in a time scale of the order of 50 fs or so.

Thus, measurements of DXS for superconductors could lead to observation of these Cooper-pair resonance processes and their dependence on center-of-mass momentum q. It is important to note, however, that this signal would be sitting on a large background of inelastic phonon scattering and disorder scattering (for an imperfect crystal) where intensity would scale as the total atomic number per unit cell, Z, of the crystal. Cooper-pair charge density, on the other hand, would carry strength corresponding to the Thompson cross section of less than one electron per unit cell, and hence would be at least a factor $1/Z$ weaker. (The actual amplitude will depend on the fraction of the conduction electrons taking part in pairing. This would be largest in the high T_c cuprate superconductors.) Hence, one expects that the very high photon flux per pulse at the LCLS would play a critical role in enabling this class of experiment.

It should be noted, however, that this kind of energy resolution is already becoming available in inelastic X-ray scattering at third-generation light sources. Thus, the use of fast DXS measurements would probably start to be competitive at still lower energy scales in the meV range.

9. Comparison of the LCLS with slow neutron sources for measurement of low-energy excitations

As discussed above, use of the DXS technique on a FEL source such as the LCLS has the potential for studying excitations in matter with periods in the microsecond to picosecond time range. Inelastic neutron scattering experiments typically measure frequencies in the $\hbar\omega \sim 1$–100 K (*i.e.* in the 100 GHz to 100 THz) range. Experiments at the LCLS would overlap the low-frequency end of this range and extend it down into the tens of megahertz domain. Since X-ray scattering couples to charge density rather than spin density, the information provided would be complementary to that coming from the neutron scattering measurements. Another complementarity comes from the fact that X-ray scattering is strongest from high-Z elements while neutrons are particularly useful for hydrogen scattering measurements. It seems likely that availability of the LCLS could therefore open up an area of study of the properties of matter paralleling, and in many ways complementing, those accessible to slow neutron scattering spectroscopy.

10. Laser-induced X-ray parametric scattering

The idea of using a pulsed X-ray beam from a FEL-type device to study excitations produced by a laser field at IR or optical frequencies in a crystalline sample is an interesting one. In its simplest form it has recently been tested by Coppens and collaborators (White, Pressprich, Coppens & Coppens, 1994). In this experiment a laser pulse is used to excite a long-lived fluorescent state in an aromatic molecule and the resulting change in molecular scattering factor is measured at the Bragg peaks. By subtracting out the background diffraction using a phase-locked detection scheme, sensitivities of better than 1% can be achieved (*i.e.* a measurement can be made even if only 1% of the molecules are excited).

Eisenberger (1994) has suggested a different version of this experiment in which photons with wavevector $\mathbf{q}$ of the laser beam cause a stimulated Raman scattering of the X-ray beam off the crystal Bragg condition. In order to measure q-dependent properties of the laser-induced excitations (at optical wavelengths only though), one needs to perform the experiment with good energy resolution of the incident and scattered X-rays. This is because a given scattering event in which incoming X-rays with wavevector $\mathbf{K}_0$ are scattered to $\mathbf{K}_1 = \mathbf{K}_0 + \mathbf{q}$ will include both excitation absorption (stimulated Raman) events and excitation scattering (stimulated Brillouin), and to discriminate one from the other requires good energy-resolution analysis of the scattered X-rays.

This can be seen in terms of Feynman diagrams, as shown in Fig. 1. Because the Raman and Brillouin processes have the same matrix elements, the only way to distinguish them is through their energy-loss profiles in the scattered X-ray beam. In the stimulated Raman event the energy gain will be precisely that of the injected laser photon, while the Brillouin processes will lead to scattering at all $\mathbf{K}_1$ and thus lead to a continuum in the energy-gain spectrum. In particular, the limit for which $\mathbf{K}_1 - \mathbf{K}_0$ = a Bragg vector would include Coppens' experiments where the X-ray scattering is quasi-elastic. In this limit all the injected energy ends up in the crystal and none in the scattered X-ray beam.

It should be noted that the cross section for scattering off-resonance is extremely small so that such experiments would only work at either an absorption line for the laser photons or for the X-ray photons. For the laser photon resonance one needs to find a narrow absorption line, since the resonant enhancement of the cross section is proportional to $(\omega/\gamma)^4$, where ω is the resonant absorption frequency and γ is its line width. For propagation of modes at the laser frequency, this means one is restricted to rather sharp exciton-like levels which lead to polariton modes when coupled to the electromagnetic field. It is these same relatively long-lived exciton-like levels which may also be observed in their relaxed state as in Coppens' experiments. The new aspect of the Raman measurements is the fact that one can look at the dispersion of the polariton modes, which can potentially give information about the rates of energy transfer from one molecule to another.

For measurements of this type, the resolution requirements both in q space (transverse coherence) and in ω space (longitudinal coherence) are quite restrictive. An X-ray FEL source of the LCLS variety would therefore have

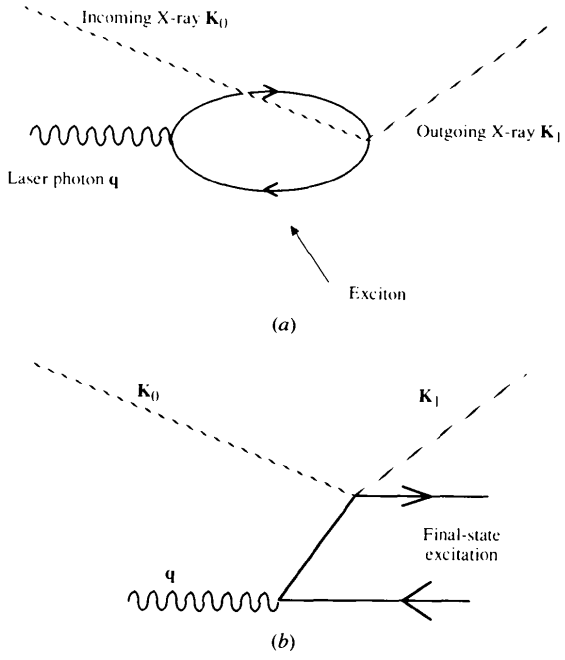

Figure 1
(*a*) Stimulated Raman diagram. (*b*) Stimulated Brillouin diagram.

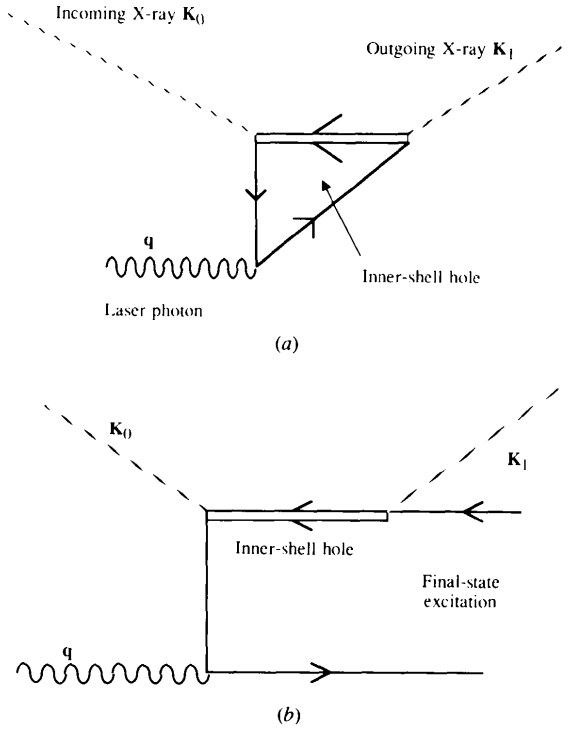

Figure 2
(*a*) Stimulated Raman diagram involving a core hole. (*b*) Stimulated Brillouin diagram involving a core hole.

considerable advantages over undulator sources. However, the number of problems where the Raman measurements lead to significant new information relative to the relaxed-state measurements may be quite limited.

Laser-induced modifications of X-ray resonant scattering (*i.e.* close to an inner-shell absorption edge) could lead to interesting effects, as reported by Namikawa, Uematsu, Zhang, Ando & Itoh (1994) for a gadolinium crystal. Here, an X-ray photon is absorbed, then the resulting inner-shell valence electron excitation is modified by a laser photon leading to a q-shifted X-ray fluorescent line. The Feynman diagrams for this case are shown in Fig. 2.

As in the off-resonance events, both Raman and Brillouin scattering should occur. In this experiment the X-rays were monochromatic with energy resolution of 2 eV, so that advantage could be taken of the resonance condition: off-resonance events of the Brillouin type will have lower cross section. Namikawa *et al.* (1994) did observe a peak (after background subtraction) at the Raman wavevector $\mathbf{K}_1 = \mathbf{K}_0 + \mathbf{q}$, indicating that two-wave mixing did occur. They report a cross section $\sim 10^{-3}$ of the one-photon value (presumably per laser photon).

Following this example from the point of view of experiments at the LCLS, one would need to monochromate the photon pulse in order to resolve the Raman from Brillouin processes in X-ray absorption-edge resonance experiments. Since total flux comparisons with X-ray undulator beams are on a per-bandwidth basis, the LCLS will keep its 10^4-fold advantage for fast pulse experiments even after monochromation. Similarly, X-ray structure-factor measurements at optical absorption lines (*i.e.* of the Coppens type) will be able to take advantage of the time structure of the LCLS to observe short-lived resonances with much shorter lifetimes, perhaps down to the order of picoseconds, compared with analogous experiments using synchrotron X-ray undulator sources. Since one LCLS pulse is worth 10^4 undulator pulses, and assuming that the laser repetition rate is the same as the LCLS repetition rate, observation of any excited state whose lifetime is shorter than the time needed for $\sim 10^4$ synchrotron bunches, *i.e.* of the order of 10 ms, will have an advantage at the LCLS.

The degree of advantage will depend on degradation of the sample due to damage both from the X-ray photons and the laser photons, since signal averaging at the undulator can, in principle, make up for the peak intensity disadvantage until it is killed by sample degradation.

The author wishes to thank Roman Tatchyn, Herman Winick, Hudel Luecke, Z.-X. Shen and George Brown for help and stimulating discussions. He is grateful to Artie Bienenstock for a suggestion which lead to this work. Partial support from the Department of Energy through SSRL is gratefully acknowledged.

References

Arthur, J., Materlik, G., Tatchyn, A. R. & Winick, H. (1995). *Rev. Sci. Instrum.* **66**, 1987–1989.

Arthur, J., Materlik, G. & Winick, H. (1994). Organizers. *Workshop on Scientific Applications of Coherent X-rays*. SLAC Report 437. Stanford Linear Accelerator Center, Sand Hill Road, Menlo Park, CA 94025, USA.

Berne, B. J. & Pecora, R. (1990). *Dynamic Light Scattering with Applications to Chemistry, Biology and Physics*. Malabar, Florida: R. E. Krieger.

Bonifacio, R., De Salvo, L., Pierini, P., Piovella, N. & Pellegrini, C. (1994). *Phys. Rev. Lett.* **73**, 70–73.

Brauer, S., Stephenson, G. B., Sutton, M., Bruning, R., Dufresne, E., Mochrie, S. G. J., Grubel, G., Als-Nielsen, J. & Abernathy, D. L. (1995). *Phys. Rev. Lett.* **74**, 2010–2013.

Demler, E. & Zhang, S. C. (1995). *Phys. Rev. Lett.* **75**, 4126–4129.

Eisenberger, P. (1994). *Workshop on Scientific Applications of Coherent X-rays*, SLAC Report 437, p. 107.

Farago, B., Monkenbusch, M., Richter, D., Huang, J. S., Fetters, L. J. & Gast, A. P. (1993). *Phys. Rev. Lett.* **71**, 1015–1018.

Gog, T., Len, P. M., Materlik, G., Bahr, D., Fadley, C. S. & Sanchez-Hanke, C. (1996). *Phys. Rev. Lett.* **76**, 3132–3135.

Kirz, J., Ade, H., Anderson, E., Buckley, C., Chapman, H., Howells, M., Jacobsen, C., Ko, C.-H., Lindaas, S., Sayre, D., Williams, S., Wirick, S. & Zhang, X. (1994). *Nucl. Instrum. Methods*, B**87**, 92–97.

Lindaas, S., Jacobsen, C., Howells, M. & Frank, K. (1992). *Proc. SPIE*, **1741**, 213–222.

London, R. A., Trebes, J. E. & Jacobsen, C. J. (1992). *Proc. SPIE*, **1741**, 333–340.

Mahendrasingam, A., Martin, C., Fuller, W., Blundell, D. J., MacKerron, D., Rule, R. J., Oldman, R. J., Liggat, J., Riekel, C. & Engström, P. (1995). *J. Synchrotron Rad.* **2**, 308–311.

More, R. M., Zinamon, Z., Warren, K. H., Falcone, R. & Murnane, M. (1988). *J. Phys. (Paris) Colloq.* **49**, 43–51.

Namikawa, K., Uematsu, H. K., Zhang, X. W., Ando, M. & Itoh, S. (1994). *Workshop on Scientific Applications of Coherent X-rays*, SLAC Report 437, p. 133.

Rossbach, J. (1996). *Coherent X-ray Sources as a Part of a Linear Collider Design*. DESY Report. http://info.desy.de/pub/hasylab/xfellit.html

Rozmus, W., Tikhonchuk, V. T. & Cauble, R. (1996). *Phys. Plasmas*, **3**, 360–367.

Solem, J. C. & Baldwin, G. C. (1982). *Science*, **218**, 229–235.

Solem, J. C., Boyer, K., Haddad, W. & Rhodes, C. K. (1990). *Proc. SPIE*, **1227**, 105–115.

Sutton, M., Mochrie, S. G. J., Greytak, T., Nagler, S. E., Berman, L. E., Held, G. A. & Stephenson, G. B. (1991). *Nature (London)*, **352**, 608–610.

Tegze, M. & Faigel, G. (1996). *Nature (London)*, **380**, 49–51.

White, M. A., Pressprich, M. R., Coppens, P. & Coppens, D. D. (1994). *J. Appl. Cryst.* **27**, 727–732.

Williams, S., Causgrove, T. P., Gilmanshin, R., Fang, K. S., Callender, R. H., Woodruff, W. H. & Dyer, R. B. (1996). *Biochemistry*, **35**, 691–697.